

Assessment of the Lidar topographic technique over a coastal area

Jacques Populus*, Gerald Barreau**, Jacques Fazilleau***,
Michel Kerdreux*, Jacky L'Yavanc*

* Ifremer, BP 70, 29280 Plouzané, France, jpopulus@ifremer.fr

** Present address: 7 champ de Bazeille, 33240 Lalande de Fronsac

*** DDE Service Maritime, 16 rue du Sénégal, BP2042, 17000 La Rochelle

Abstract

The lack of adequate topographic data for tidal flats and saltmarshes currently hinders both physical and biological inventories and fine mesh hydrological modelling. Lidar altimetry offers a way of bridging the gap left by hydrographers. The purpose of this paper is to assess the Lidar results of an airborne campaign conducted in spring 2000 over the Anse de l'Aiguillon, France. Two recent data sets are available, a classic depth survey acquired six months earlier and a recent transect carried out with centimetric dGPS. Comparisons of co-located samples are performed and discussed.

Over saltmarshes, a Spot image is used to classify the main vegetation units in terms of height and density. An attempt is then made to infer, from signal dispersion levels, the true height at which the Lidar signal was generated. A composite digital terrain model is then generated, using Lidar data completed by depth soundings. Geostatistics are used for interpolation with a 5 metre output mesh size. The quality of the model and of the isocontours is discussed. An overall cost assessment and methodological tips are given as well as a conclusion on the prospective use of this technique.

Résumé

Le manque de données topographiques sur les estrans et marais maritimes rend difficiles les inventaires biophysiques et la modélisation hydrodynamique à maille fine. L'altimétrie par laser aéroporté offre aujourd'hui une solution pour combler ce vide. Cet article se propose d'évaluer les résultats d'une campagne aéroportée conduite au printemps 2000 dans la baie de l'Aiguillon, en Charente-Maritime, France. Deux jeux de données récents sont disponibles, un levé bathymétrique classique ainsi qu'un profil au sol acquis au dGPS centimétrique. Une comparaison est effectuée entre points voisins et les résultats commentés.

Pour filtrer l'effet des végétations de schorre, une image Spot est utilisée. Les principaux groupements sont classés en termes de hauteur et densité. La dispersion du signal Lidar est calculée pour chaque classe, permettant une hypothèse sur le niveau de génération du signal.

Un modèle numérique de terrain complet est produit sur une maille de cinq mètres par interpolation géostatistique. La qualité du MNT et des lignes de niveau est discutée ainsi que les apports au plan géomorphologique par rapport aux seules données bathymétriques. Enfin, des détails méthodologiques, une estimation des coûts ainsi que les perspectives d'utilisation de cette technique sont donnés.

Introduction

The Lidar technique has been used for a few years in various thematic fields, e.g. topography and hydrography (Ritchie, 1995; Krabill et al., 1994), forestry (Kraus, 1997), volcanology and civil engineering. In the Netherlands for instance, extensive coverage of the country including the coastal zone (Van de Kraats, 1999) has recently been achieved. The need for accurate ground topography is particularly strong when water flow is concerned, i.e., in orography, as well as in the coastal zone. Traditional hydrographic techniques have been successful so far in mapping the obstructions to navigation found in the tidal zone, using classic sounders wherever possible, with the help of aerial photography. In general, not much concern has been shown for low lying sedimentary shorelines, as they are of little interest to navigators.

Only recently, under the pressure of environmental and impact studies, has a new concern arisen about the need for more accurate description of tidal zones and shorelines. This is true in places prone to erosion or where exceptional water level rise or other hazards entail damages to coastal properties. Both knowledge and quantification of deposition processes and progress in hydrodynamic modelling require better knowledge of bottom topography. Accuracy comparable to that of classic depth sounding, i.e. around 10 cm, is sought. Traditional photogrammetry falls short of this requirement, unless using very high scale aerial photos (around 1 / 4000). Roving dGPS is also a new method that derived from exceptional progress in global positioning. However, when exhaustive mapping is required, these two techniques are extremely time consuming and costly. This has paved the way for Lidar topographic mapping.

The topographic Lidar technique

Main Lidar features

The main features of the Lidar technique have been described by a number of authors. The topographic Lidar emits pulses of light in the near infra-red range (typically around 1 to 1.5 μm). Their interaction with ground targets modifies their frequency, intensity and phase. The measurement of the time lapse between emission and return provide a way of knowing the distance between instrument and ground (Samberg, 1997; Measures, 1997). The most up to date technique is a laser source with frequencies from 2000 to 80000 Hz going to a scanning mirror, providing a typical swath of 70% of altitude. It is associated with a dGPS and an Inertial Navigation System (INS). The dual bi-frequency dGPS acquires aircraft and ground station positions every second (1Hz), yielding the aircraft position with 3cm accuracy after post-processing. By recording aircraft movements, the INS controls acquisition geometry at high frequencies. INS and GPS are coupled with a Kalman filter (Fritsch, 1993), thereby combining their respective advantages, GPS stability and INS high instantaneous precision.

A study of systematic and random errors of topographic Lidar measurements made by Huising (1998) reports an overall error ranging from 10 to 200 cm, depending on terrain type, slope and roughness. In the case of tidal flats, precision of 10 to 20 cm can be expected.

Operational tips and constraints

Preparation of a survey involves the following points:

- acquisition is either by day or night, the latter providing better GPS conditions. The flight plan is similar to that of a classic aerial survey. 40% overlap between flight lines must be ensured to provide proper geo-referencing (Lemmens, 1997). Of course, for tidal zone acquisitions, these flight lines must be positioned with respect to the varying water levels.

Operation time is therefore reduced to a few hours around low water. Typically, the surface range covered per hour is between 20 and 30 km².

- the dGPS ground station should not be more than 15 km away from the aircraft at all times, in order to keep dual GPS paths identical. Positioning deteriorates rapidly with longer baselines.

- reference zones of approximately one hectare must be ground surveyed prior to the flight, using centimetric dGPS. They should be within the periphery of the Lidar surveyed area, and no further than 10 km away from any surveyed point (figure 1). A few more reference zones may be surveyed for validation purposes.

- point density must be chosen in view of user needs. For given instrument features, this will determine flight altitude and hence cloud ceiling constraints. However, most systems do not operate higher than 1000 metres due to pulse energy limitations. Typically, one point for 4 m² is achieved.

Depending on the type of instrument, either the first or the last pulse or both can be recorded. While most applications are aimed at building a Digital Terrain Model (DTM), some are concerned with objects above ground surface, e.g. vegetation or human constructions (Digital Elevation Model: DEM). Data pre-processing is mostly based on filtering but also requires operator-assisted procedures in order to provide both first pulse and last pulse files. However, pulses less than 3 nanoseconds apart (1 metre on the ground) cannot be separated, making it difficult to identify low lying vegetation for instance. A thorough description of the features of various systems can be found in Huisling (1998).

Processing methods and tools

Data pre-processing and analysis tools

The result of a Lidar acquisition may be delivered by an operator as a DTM with a given cell size. However, most users want to be able to "zoom in" and get a more detailed view of a given area by adapting the cell size. Lidar files usually contain millions of X,Y,Z ASCII records which common desktop software programs cannot handle. In this project, two types of files were ordered from the operator. These were a) the original ASCII file after nominal filtering (i.e., containing the last pulse insofar as possible), b) a reduced X,Y,Z ASCII file after specific filtering which decreased its size by an order of magnitude.

The Lidar files were delivered in the UTM projection system, which was chosen as the reference system for all other data files. All ground data, usually collected in the local French Lambert system, were transformed to UTM using the Esri Arcview GIS. Since a Spot image was also processed, Erdas Imagine software was also utilized. After being made compatible, all files were imported to Isatis (Géovariances, France), special spatial interpolation software that contains many modules for examining both spatial and statistical data. In particular, a tool called "migration" can be used to select points from given files and flag them according to specific conditions of proximity. This tool was extensively used to validate Lidar measurements against ground truth files.

The sequence of operations carried out for data processing consisted of:

- data reading, geo-referencing of plane coordinates, shift on the Z coordinate
- interactive elimination of the underwater sections
- computing statistics, seeking and eliminating duplicates and outliers
- "migration" and flagging of pairs of points
- image classification, statistics by moving window
- correlations and spatial display.

Digital terrain model production method and tools

Once the Lidar file was ready, interpolation could be performed. Regional structural analysis, also termed "kriging" was applied with the Isatis software. Variographic analysis and modelling are amply described in the literature (Armstrong, 1986). Although more specifically useful for irregular measurement distributions, kriging still gives better results than other interpolators for regular distributions (as is the case here) when cell size becomes smaller than the mean inter-measurement distance (Sanchez, 1999). Kriging may be used with Isatis for the following reasons:

- possibility of dealing with anisotropy, i.e. regional structures which vary with the azimuth,
- thorough parameterizing of the neighbouring window, to look for samples in all directions,
- best reliability of the interpolation over areas devoid of measurements (e.g. small pools in the intertidal zone)
- computation of the interpolation variance for each output cell, an indicator of its reliability.

Acquisition survey over the Anse de l'Aiguillon, France

Study site and available data

The Anse de l'Aiguillon is located in Charente-Maritime, on the central Atlantic coast of France. Stretching between the Aiguillon and Saint-Clément headlands, this 40 km² bay is mostly composed of tidal flats ("slikke") occupied in the lower levels by shellfish farming activities (mostly mussel poles), whose leased areas are shown in figure 1. Although it is extremely flat (with slopes generally less than 1%), the slikke exhibits numerous secondary channels and micro-structures called "ruissons" that originate on higher levels and drain seawater during ebb tide. Their slopes can be sharper in limited areas.

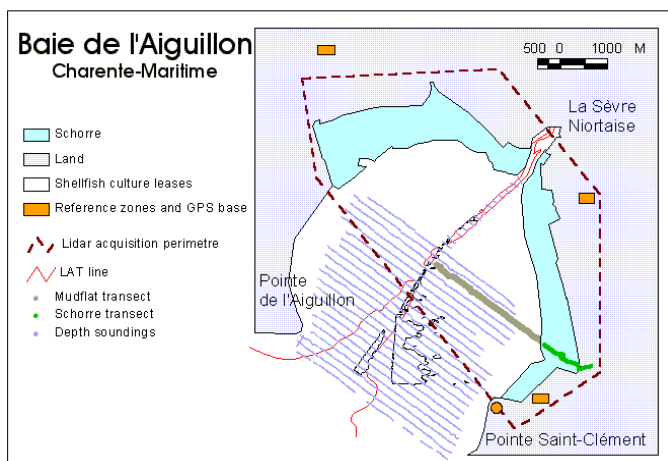


Figure 1: study site of Baie de l'Aiguillon, Charente-Maritime, France.

The upper part is occupied by saltmarshes ("schorres") that are coded light green in figure 1. They can be clearly seen on the Spot image of figure 2. This image has been colour enhanced over the schorre area only. The halophyte vegetation has developed with respect to the micro-relief and water drainage efficiency (Guillaumont, 1991). Going upwards from the slikke, at first there are only clumps of pioneering *Spartina*, then the vegetation becomes denser with combinations of *Aster*, *Sueda* and *Spartina* on soils with abundant residual water. On the upper levels, *Obione* (darker blue) form dense covers of constant height of about 40 cm all year round, on well drained terrain. The graminea *Agropyrum* (lighter pink), which is quite dense and can reach 70 cm at its highest in summer, is usually found on the upper levels and harvested for fodder. A number of permanent very shallow pools remain. These will generate Lidar light absorption and hence gaps in the data. They appear as darker patches on the image. Saltmarshes are limited landward by dykes approximately 3 metres high, which protect the polders from invasion by the sea.



Figure 2: Spot 4 image, 5 May 2000, colour composite of channels green, red, MIR.

The Spot4 image in figure 2, with a resolution of 20 metres, was acquired on May 5th, the same day as the Lidar survey, at 10.50 GMT, i.e. 20 minutes before low water.

The LAT line is shown in red in figure 1. The maximum tidal amplitude in the bay is around 6.5 metres. The Sèvre river's channel never dries out. Figure 1 also shows in blue the distribution of depth soundings performed by the local coastal administration (DDE) during the winter of 1999/2000. They hardly reach 4 metres above LAT, because surveys are hindered by both the flat topography and mussel poles occupying the channel banks. These soundings followed the typical bathymetric protocol of 1 / 20 000, i.e., one sounding every 20 metres on profiles 200 metres apart. Their accuracy is currently estimated at 10 cm. As can be seen, a good 40% of the bay's tidal area remains

unsurveyed by classic soundings. In spring 2000, the DDE also performed a dGPS field transect at high water, by using a dinghy to tow a sled on which the dGPS antenna had been fitted. This transect, extending all the way from the channel to the dyke across both slikke and schorre, samples true ground level every metre. It is coded grey over the slikke and green over the schorre in figure 1. It will be used below in the validation process.

Geodetic aspects

Lidar data were acquired directly in X,Y,Z UTM, with the Z component expressed as an altitude above the IAG GRS80 ellipsoid.

In order to be as close as possible to the site, the fixed dGPS station was installed on the Saint-Clément headland (figure 1), a reference point commonly used by local surveyors. As this station initially was not referenced to the IAG GRS80 ellipsoid, it had to be linked to a point 15 km away belonging to the French national geodetic network. All data from the DDE, i.e., ground transects and depth soundings had been acquired for practical reasons with reference to the LAT at Saint-Clement, itself locally linked to the IGN69, the national altitude reference, by a tidal gauge in nearby La Pallice harbour. The link was then complete between the LAT and the IAG-GRS80. It should be added that only small residual errors may result from the variation of the LAT between our site and La Pallice 10 km away.

Data acquisition, pre-processing and delivery

Relying on a real-time weather forecast beginning a few days before the peak spring tide, the operator was on stand-by with its high-wing single-engined Cessna carrying the ALTM 1020 Lidar system. On May 5th, they started acquisition 1h30 before low water (0.76 m tide height) going down from the most landward flight line and finished 40 minutes after low water (1.13 m). At a flight altitude of 700 metres, 21 lines of 480 metres, with 40% overlap were necessary to cover the site (surveyed area shown as dotted line in figure 1). The ground dGPS

data acquired during the flight were provided to the operator for post-processing. The operator then performed nominal pre-processing according to the specifications (8 cm on Z) in order to attain the best possible overall accuracy, while eliminating outliers and dubious measurements. Upon our request, all points with a Z value more than one metre away from surrounding points were eliminated. This only concerned houses and trees, outside of the scope of the study. Measurement density had been specified as one point per nine square metres. In fact, as 1 point per four square metres was achieved in overlapping zones, the specifications were exceeded. Upon our request, three products were delivered: a) the original file containing 10^7 points in ASCII form (approx. size 350 MO), b) a reduced file obtained by filtering according to the following rule: within a 5 metre radius circle around each measurement point, elimination of all points with a Z difference less than 30 cm. The resulting point number dropped to 10^6 , c) a 10 metre cell DTM made by simple averaging within each cell.

Results and discussion

Lidar assessment compared to a dGPS transect on bare tidal flats

In the following section, the ground transect mentioned above and shown in figure 1 is referred to as absolute altitude reference, in spite of the slight error affecting even the best centimetric dGPS measurements. The Lidar data are then considered as one particular realisation of this true altitude. The comparison was performed by sub-setting the original Lidar file over the same zone as the field transect (limited to its tidal flat part, i.e., 2600 regularly spaced points). Once imported into Isatis, the migration procedure was applied to the two files as follows: for each transect point, the software searched the Lidar subset file for points within a given distance. Two sets of pairs (z_{ground} , z_{lidar}) were thereby formed, set#1 with 283 pairs of points no more than 0.5 metres apart, and set#2 with only 50 pairs within 0.2 metres. The statistics of $z_{ground}-z_{lidar}$ are shown in table 1.

Table 1: statistics of Lidar versus dGPS ground measurements and soundings (in parenthesis the colocation distance value in metres)

Variable	Count	Minimum	Maximum	Mean	Std. Dev.
$z_{ground}-z_{lidar}$ (0.5m)	283	- 0.23	0.61	- 0.01	0.11
$z_{ground}-z_{lidar}$ (0.2m)	50	- 0.23	0.22	- 0.006	0.10
$z_{ground}-z_{sounding}$ (4 m)	71	-0.19	0.14	0.05	0.05
$z_{lidar}-z_{sounding}$ (1 m)	341	-0.45	0.50	0.02	0.16

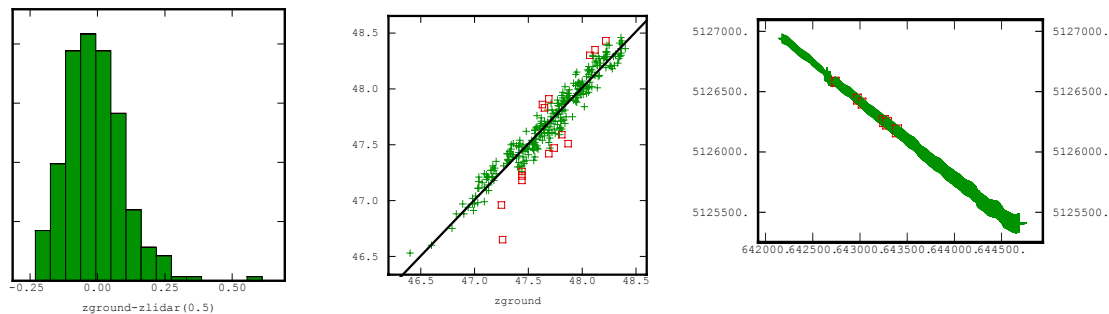


Figure 3 : a) histogram of $z_{ground}-z_{lidar}$, b) scatter plot of $z_{ground}-z_{lidar}$, with red squares for outliers, c) locations of outliers in the transect

Figure 3a shows that the distribution is Gaussian. It comes out that the mean difference is negative (the Lidar measures above the ground) and that the accuracy of the Lidar is better than 1 cm, whereas its precision (standard deviation SD1 of the differences) is 11 cm. When a closer migration of 0.2 m is performed, these figures hardly change at all.

The correlation shown in figure 2b has a coefficient of 0.96. Figure 2b also highlights the outliers in red. The locations of these outliers on the ground (figure 2c) do not reveal any particular pattern. They are probably generated by highly localized ruggedness.

Soundings assessment compared to the dGPS transect and Lidar data

Depth soundings are just another realisation of true altitude, with a precision currently estimated by local hydrographers as being 10 cm. Since these soundings were partly carried out in Dec. 1999, that is, before the exceptional storms that affected the region, they should be considered with caution. Yet it seemed interesting to compare these soundings with ground transect values. To have a sufficient number of samples (71, table 1), we had to increase the migration distance to 4 metres. With a slope along the transect of 0.5%, this may only generate a random topographic signal of 2 cm. Table 1 shows that soundings read on average 5 cm below the actual ground surface. This could be explained by a siltation trend since the storms in winter 1999/2000. The standard deviation of 5 cm is very low, when compared to the 10 cm precision currently given for sounding.

Finally, we looked at the Lidar values compared to depth soundings of a larger test area extending from the upper slikke across the channel. For a migration value of one metre, 341 pairs were available, denoting an average difference of 2 cm and a standard deviation of 16 cm. The Lidar probably gives a higher ground reading. It is difficult to interpret this result any further in terms of bias, as some elements are out of control. For instance, the geoid height above the ellipsoid, which was used to connect the ellipsoid to the LAT, may also account for a couple of centimetres of bias.

The discussion on deviations is more straightforward. The two above assessments can be interpreted in the following way, in terms of variance. Assuming that the ground reference transect is the true altitude, we can consider that we measure this altitude by two separate methods, Lidar with a SD1 of 11 cm (variance 121) and sounding with SD2 equal to 10 cm (as per soundings specifications). When the two measurements are compared, the total expected variance should be:

$SD3^2 = \sqrt{(SD2^2 + SD1^2)}$, yielding a value of 15 cm, close to that above of 16 cm.

These results do validate the Lidar technique. The accuracy of just a few centimetres is very good and the precision of around 10 cm on bare soil without relief has been achieved, as also reported by Huising (1998). Clearly, precision will be lower when the terrain type generates noise, as is the case with vegetation and slope.

Influence of saltmarsh vegetation on Lidar measurements

As described above, on low lying vegetation, there is no way of getting both the front and rear pulses of the Lidar signal. There is no a priori way of knowing where any given Lidar pulse will be reflected, i.e. at the top of the vegetation or anywhere between there and the ground. In order to retrieve the ground level, we can try to record the lowest altitude, taking for granted that it is closest to true ground, but this is still uncertain.

In general, schorre vegetation height and density are rather well correlated. However, the shape of their canopy may induce varying behaviour of the laser beam hitting them. In the

present case, the laser beam's footprint is 20 cm in diameter. On dense Obione cover (40 cm high) for instance, the return pulse shape may be rather clean. Conversely, on the graminea Agropyrum, which can reach 60 cm and grows in clumps on the upper part of the schorre, some Lidar pulses may actually reach levels close to the ground and the resulting pulse will be quite different between two close locations.

In order to address this behaviour, the schorre area of the bay was mapped using the Spot image. Ground truth collection had been carried out during the overflight period. Basically, five classes were identified, with emphasis on the two with taller vegetation. The result of the classification is given in figure 5 for the northwest part of the bay.

By measuring signal dispersion on a moving window, we could at least have an idea of the signal accuracy degradation induced by the vegetation. Choosing a 10*10 m² window size, an average of 23 samples is taken and the topography's influence remains low (slopes being no more than a few per thousands). The standard deviation of Lidar measurements was computed under Isatis. The resulting file (10 metre mesh size) was exported to Arcview and standard deviations then averaged per vegetation class, using a « summarizing » function. The results are shown in figure 6. As expected, the dispersion on mudflats is close to that found above.

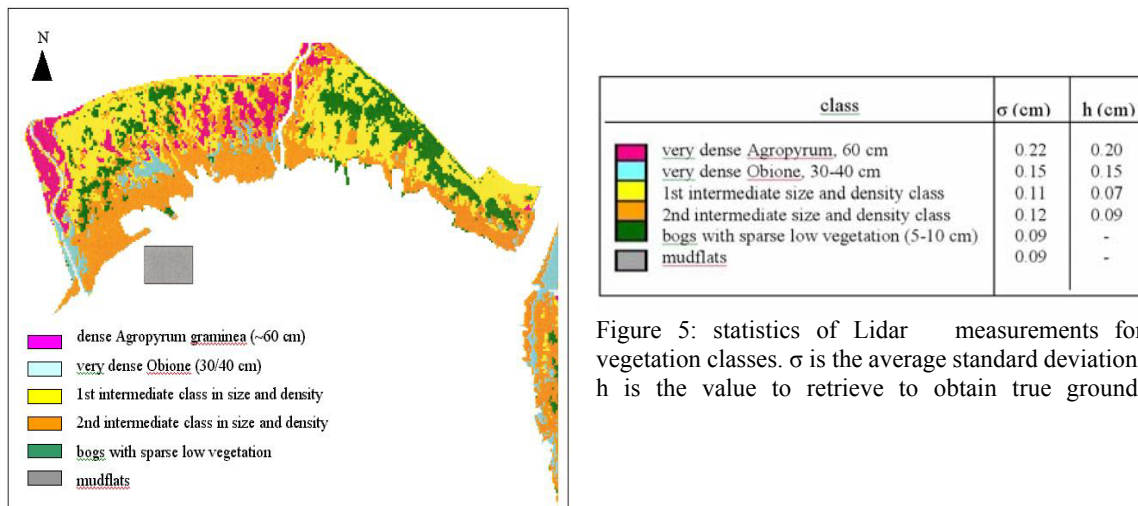


Figure 4: supervised classification of Spot image over the northwest schorre area.

Figure 5: statistics of Lidar measurements for vegetation classes. σ is the average standard deviation, h is the value to retrieve to obtain true ground.

As vegetation height and density both increase, dispersion also increases up to 0.22 metres. It can be concluded that the presence of Agropyrum increases the noise level by 0.20 m, that of Obione by 0.15 m. Therefore, for an initial approximation it is suggested that these values (given in the last column of figure 6) be retrieved from Lidar measurements on a per class basis in order to best approach the true ground level. In other terms, this corresponds to roughly half the canopy height of the given vegetation class.

In conclusion, once time gating is improved, the possibility of detecting the last pulse will allow true ground to be mapped, although measurements yielded are bound to be scarce. Fortunately in the present case, the extremely low ground declivity did not require dense measurements.

DEMs generation

The variographic analysis and modelling parameters

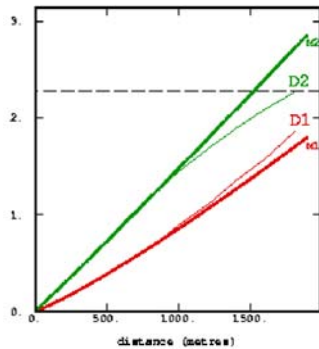


Figure 6: bi-directional variogram of Lidar data

For practical reasons, the variographic analysis is performed on only a subset of the entire file at full resolution. After anisotropy directions have been sought out, only the two variograms showing the largest differences are kept, as shown in figure 6. The sharpest variation appears in trigonometric azimuth 135° and the slowest in azimuth 45° , which is consistent with the general slope line of the area. The model is then built as a sum of two curves which are parameterized to reproduce these two variograms. A slight nugget of 2 cm is set at the origin, to smooth measurement error. The neighbourhood is divided into 8 sectors. Only one of which can be empty, which restricts interpolation along borders. So that no hole is left in the output grid file, the radius is set to the appropriate value (roughly half the largest “hole” size). The

output cell size is defined on two scales. A five metre cell is chosen to produce a synoptic DEM of the whole area with the reduced data file. It provides a basis for comparison with a DEM built using classic soundings. A one metre cell is also used to illustrate the full value of the interpolated Lidar data on specific zoomed areas.

Geomorphologic discussion

Figure 7 shows a subset area of the lower Sèvre channel on a 5 m cell DEM built up with Lidar data and a 20 m cell DEM with sounding data. Colours are spaced 0.2 m and contours 0.5 m and span the 42-48 m elevations (heights under 43.46 m come from the soundings file on both models).

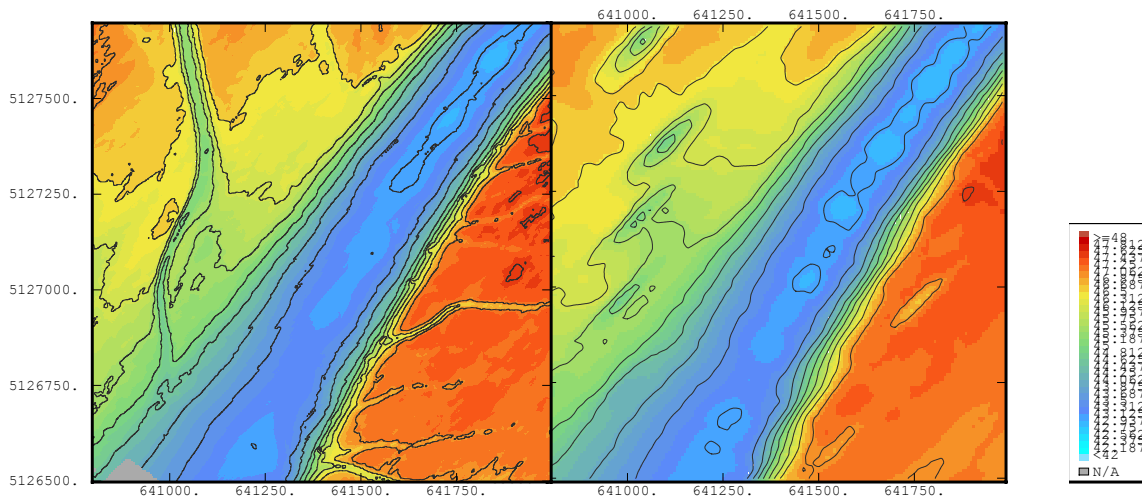


Figure 7: Comparison of the DEM on lower bay reaches a) 5 m cell Lidar, b) 20 m cell soundings (coordinates in metres)

Lidar data clearly show the main secondary channel on the left hand side, which the soundings only catch when their profiles intersect it and represent as holes. This could be

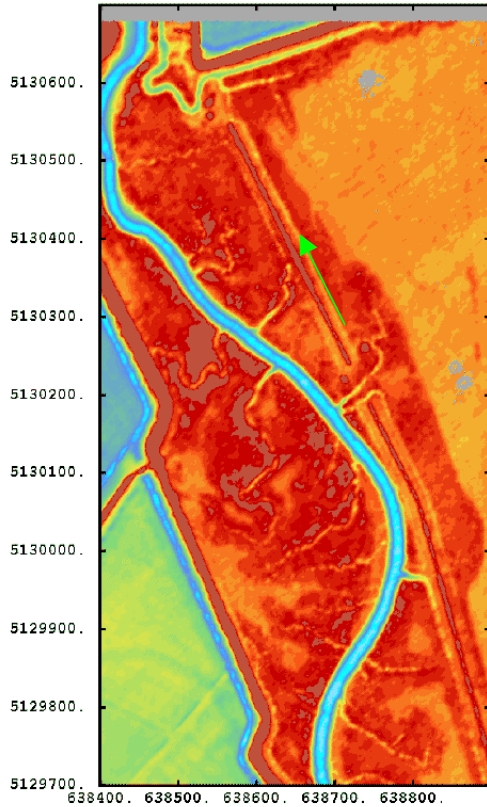


Figure 8: at left, the NW schorre DEM, resolution 1 metre (coordinates are in metres), above ground picture looking NNW (see green arrow)

expected in view of the 200 m spacing between these profiles. Similarly, a host of micro-channels up to one metre deep can be noticed on the right hand side.

Figure 8 left shows the northwest schorre area mapped on a one metre cell, giving the full resolution of the data, colour spaced every 10 cm between 47 m and 50 m heights. Landward,

the area is bordered by a 3 m high dyke protecting the lower lying polders behind (blue-grey and green tones). To illustrate the vertical resolution, the picture in figure top looks NNW towards the dyke's corner. A trough of Obione along a small drainage channel, about 4-5 metre wide on the picture's axis, runs between two banks of graminea. It appears in orange/yellow against red tones on the DEM. Furthermore, a former eroded dyke a couple of feet high is seen at the very left of the picture, where graminea are mixed with other higher terrain halophyte plants. It runs as a brown straight line on the DEM. Note that no noise is visible on the DEM, even though the vertical resolution is on the same order as the measurement standard deviation (11 cm). Of course, for these elevations to show ground level, a correction should be applied using fine knowledge of the vegetation distribution, according to the section above.

Figure 9 a) is another DEM (one metre cell) in the eastern part of the bay. It is compared to an ortho-photography dated July 1st, 1999 (i.e. two months later in the season) scanned at 0.6 metre. The model reveals all micro-channels very accurately. It gives a better result than the photography as it gives an indication of channel depth, which the former cannot do. This is striking on the bottom right "loop" channel, whose bottom is given as 49.5 m (yellow/orange) against banks of graminea reaching 50.4 m. Generally, these graminea occupy all upper channel banks, appearing as the brighter green on the picture. They are sharply enhanced in red in terms of elevation and fit quite well between both documents.

The other plants do not give any particular topographic signal, except at the lower schorre limit, where the transition to bare mudflats is well marked from orange to yellow/light green. The bog at the top centre showing up brightly (grey on Lidar DEM, i.e., no signal) is probably dry in July due to the neap tide coefficients. Likewise, the white streaks are stubble-field, graminea having probably been mown a short time before.



Figure 9: a) DEM of eastern shore (one m cell), b) IGN ortho-photography on July 1st 1999.

Conclusion

The Lidar technique has proved to be a very promising technique, especially in the coastal zone where its flexibility and non-invasiveness are extremely relevant features. Its accuracy is very satisfactory on bare ground, whereas low-lying objects (vegetation, aquaculture structures) still remain below the current level of detection. Yet this study has shown that the envelope of the higher schorre vegetation unit (graminea) is clearly denoted. In the case of above-ground objects, more subtle filtering must be carried out. In the coastal zone, this could be of interest for standing vegetation (such as mangroves) but also for human constructions, in the case of landscaping design surveys, for instance.

Current system resolutions are almost too high for some applications, such as topographic data for input into hydrodynamic models, thus leading to higher costs and unmanageable amounts of data. It is advisable to adapt the resolution to scope of each problem, to optimise the processing steps. If there are several potential applications, a reduced resolution file should be used to produce a synoptic DTM for a whole area, with a cell size ranging from 5 to 10 metres. When more detailed structures are to be shown, then the original full resolution file should be subset accordingly and zoomed DTMs computed with a smaller cell size as appropriate. Costwise, Lidar compares quite well with traditional methods. For large surveys, the cost per km² should be close to 200 US\$. In view of the not too tough weather constraints, the rapidity and accuracy of acquisition should ensure its wide success.

Acknowledgments

We would like to acknowledge the support of the CNES Isis programme, which granted us preferential conditions for the Spot image.

References

Armstrong M., 1986, Basic Geostatistics for the mining industry. Ecole Nationale Supérieure des Mines de Paris, Centre de Géostatistique, Fontainebleau.

- Fritsch D.**, 1993, Filtering and calibration of laser scanner measurements, *International Archives of Photogrammetry and Remote Sensing*, vol. 30, 379-385.
- Guillaumont, B.**, 1991, Utilisation de l'imagerie satellitaire pour les comparaisons spatiales et temporelles en zone intertidales, *Estuaries and Coasts : Spatial and Temporal Intercomparisons*, ECSA 19 Symposium, Elliot and Ducrotoy Eds, Olsen and Olsen, 63-68.
- Huising E. J., Gomes Pereira, L. M.**, 1998, Errors and accuracy estimates of laser data acquired by various laser scanning systems for topographic applications. *ISPRS Journal of Photogrammetry and Remote Sensing* 53, 245-261.
- Krabill W. B.**, 1984, Airborne laser topographic mapping results, *PE&RS*, vol. 50, num. 6, 685-694, 1984.
- Kraus K.**, 1997, Restitution of airborne laser scanner data in wooded areas, *EARSEL Advances in Remote Sensing Year Book*, vol. 5, 120-127.
- Lemmens J. P. M.**, 1997, Accurate height information from airborne laser altimetry, *ISPRS Journal of Photogrammetry and Remote Sensing*, 222-234.
- Measures R. M.**, 1997, Laser remote sensing : present status and future prospects, *SPIE*, vol. 305, 2-8.
- Ritchie J. C.**, 1995, Airborne laser altimeter measurements of landscape topography, *Remote Sensing of Environment*, vol. 53, num. 2, 91-96.
- Samberg A.**, 1997, What laser scanning can do to day : current techniques, *EARSEL Advances in Remote Sensing Year Book*, vol. 5, 114-119.
- Sanchez, J.**, 1999, Elaboration et étude critique de modèles numériques de terrain bathymétriques. *Mémoire de l'Ecole supérieure de géomètres et topographes*, Le Mans, France, 62 p.
- Van De Kraats E.**, 1999. Airborne laser scanning : an operational remote sensing technique for digital elevation mapping in coastal areas, *Geomatics and coastal environment*, Populus and Loubersac (eds), Actes de colloques, *Editions de l'Ifremer*, Brest, France, p 149-158.

Figure captions list

- Figure 1: study site of Baie de l'Aiguillon, Charente-Maritime, France
- Figure 2: Spot 4 image, 5 May 2000, colour composite of channels green, red, MIR
- Figure 3 : a) histogram of $Z_{\text{ground}}-Z_{\text{lidar}}$, b) scatter plot of $Z_{\text{ground}}-Z_{\text{lidar}}$, c) locations of outliers
- Figure 4: supervised classification of Spot image over the northwest schorre area
- Figure 5: statistics of Lidar measurements for vegetation classes. σ is the average standard deviation, h is the value to retrieve to obtain true ground
- Figure 6: bi-directional variogram of Lidar data
- Figure 7: Comparison of the DEM on lower bay reaches a) 5 m cell Lidar, b) 20 m cell soundings
- Figure 8: at left, the NW schorre DEM, resolution 1 metre, above, a picture of the area looking NNW (see green arrow)
- Figure 9: a) DEM of eastern shore (one m cell), b) IGN ortho-photography on July 1st 1999